JTTEE5 10:592-598

Lanthanum Hexaaluminate—a New Material for Atmospheric Plasma Spraying of Advanced Thermal Barrier Coatings

C. Friedrich, R. Gadow, and T. Schirmer

(Submitted 28 July 2000; in revised form 21 December 2000)

One of the main application fields of the thermal spraying process is thermal barrier coatings (TBCs). Today, partially stabilized zirconia (YSZ or MSZ) is mainly used as a TBC material. At temperatures above 1000 °C, zirconia layers age distinctively, including phenomena shrinkage and microcrack formation. Therefore, there is a considerable interest in TBCs for higher temperature applications. In this paper, lanthanum hexaaluminate, a newly developed TBC material with long-term stability up to 1400 °C, is presented. It ages significantly more slowly at these high temperatures than commercial zirconia-based TBCs. Its composition favors the formation of platelets, which prevent a densification of the coating by postsintering. It consists of La_2O_3, Al_2O_3, and MgO. Its crystal structure corresponds to a magnetoplumbite phase. Lanthanum hexaaluminate powders were produced using two different fabrication routes, one based on salts and the other one based on oxides. To optimize the granulate, various raw materials and additives were tested. The slurry was spray dried in a laboratory spray drier and calcined at 1650 °C. Using these two powders, coatings were produced by atmospheric plasma spraying (APS). The residual stresses of the coatings were measured by the hole drilling method, and the deposition process was optimized with respect to the residual stresses in the TBC. The coatings were extensively analyzed regarding phase composition, thermal expansion, and long-term stability, as well as microstructural properties.

Keywords APS, atmospheric plasma spraying, lanthanum hexaaluminate, magnetoplumbite, thermal barrier coating, thermal spraying

1. Introduction

Thermal barrier coatings (TBCs) are becoming increasingly important in several industries, primarily the aerospace industry, the automotive industry, and power plants.[3] The use of TBCs has two main objectives: on the one hand, it increases the temperature in the combustion chamber (*e.g.*, adiabatic engine concepts); and, on the other hand, it insulates materials subject to excessive temperatures and hot corrosion (*e.g.*, turbine blades). The requirements for a TBC are low thermal conductivity, high thermal shock resistance, hot corrosion protection, and long-term stability at high application temperatures.

The classic coating material is partially yttria-stabilized tetragonal zirconia (PSZ), which is applied on top of a metallurgical interlayer as a diffusion barrier and mediator of the different coefficients of thermal expansion (TBC and substrate) as well as to increase the adhesion. MCrAlYs (where M is Co or Ni) are normally used as bond coats, but aluminides or various metallurgical combinations also have been tried.[2]

There are primarily two ways to fabricate TBCs: by the thermal spray process (TS), by atmospheric plasma spraying (APS), by low-pressure plasma spraying, or, in recent years, by electron beam physical vapor deposition (EB-PVD). The EB-PVD coatings in comparison to TS coatings show an increased thermal shock resistance and a strongly reduced hot corrosion resistance, due to the lack of mechanical bonding and the presence of a columnar structure that promotes a fast oxidation of the MCrAlY bond layer. This formation of an oxide layer between the ceramic and the metallurgical interlayer leads to delamination and failure of the ceramic layer.[9] Requirements for TBCs have increased in many applications toward higher temperatures and long-term high-temperature stability (Fig. 1).

In the case of TBCs designed for long-term, high-temperature application, recent work shows that TS and EB-PVD zirconia coatings cannot fulfil the required long-term properties predicted for temperatures above 1100 °C.[1]

At temperatures above 1100 °C, most zirconia coatings show dramatic aging, including densification. The microcracks and micropores begin to heal, and the Young's modulus of the ceramic coating increases. With the increase of the Young's modulus, the tolerance for the different thermal expansion coefficients of the metal substrate and the ceramic coating decreases noticeably. Due to the decrease of porosity, thermal conductivity increases and, therefore, so does the thermal load of the substrate. Aging, postsintering, and the partial phase transformation of the zirconia TBCs from tetragonal to monoclinic lead to a dense ceramic with changed properties compared to those of the originally porous layers. In addition to the deterioration of the mechanical and thermal properties of the zirconia coating during the high thermal loads or the thermal cycling in service, another property of zirconia causes problems for long-term high-temperature use of these TBCs. Zirconia is a good oxygen ion conductor (*e.g.*, applications are the lambda sensor and the solid electrolyte in fuel cells).[7]

C. Friedrich, R. Gadow, and **T. Schirmer,** University of Stuttgart, IFKB, Stuttgart, D 70569 Germany. Contact e-mail: christian.friedrich@muc.mtu.de.

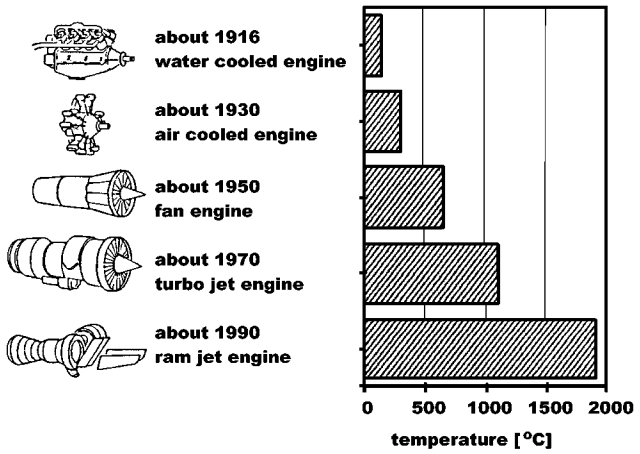

Fig. 1 Development of the combustion chamber temperature since the beginning of motorized aviation[4]

List of Acronyms	
TBC	thermal barrier coating
XRD	x-ray diffraction
CTE	coefficient of thermal expansion
PSZ	partially stabilized zirconia
TS	thermal spraying
APS	atmospheric plasma spraying
EB-PVD	electron beam physical vapor deposition
La-MP	lanthanum magnetoplumbite
PLC	programmable logic controller
BSE	backscattered electron microscopy

List of Symbols	
α	thermal expansion coefficient
c_p	heat capacity
a	thermal conductivity
ρ	density
λ	heat conductivity

At temperatures above 1100 °C, the diffusion of the neutral oxygen through the dense ceramic coating increases rapidly. Thus, oxidation of the MCrAlY interlayer is caused, as a further negative effect. In service, constant oxidation of the metallurgical interlayer takes place. The formation of the additional oxide layer leads to a volume increase and to a chipping of the ceramic coating.[9] Due to the degradation of the mechanical, thermal, and electrical properties of zirconia, these TBCs can no longer fulfil the requirements of long-term high-temperature applications, such as in stationary gas turbines.[8]

In comparison to PSZ, lanthanum aluminate shows a superior structural and thermochemical stability as well as at least equivalent thermophysical properties.[5,6] Due to the magnetoplumbite crystal structure, this material is also called lanthanum magnetoplumbite (La-MP). This layered structure (platelets) has fully occupied mirror planes because of the highly charged lanthanum cation (La^{3+}) (compare to Fig. 2) and causes effective suppression of diffusion processes vertically to the crystallographic c-axis. It is expected that the thermal conductivity in this direction is quite low as well.

Various thermomechanical and chemical properties of lanthanum magnetoplumbite already were determined.[5] A comparison of these properties with commercial zirconia TBCs is shown in Table 1 and explains the great interest in the verification of these properties for thermal-sprayed lanthanum magnetoplumbite TBCs. A La-MP powder appropriate for the atmospheric thermal spraying process was manufactured and analyzed. Using a sophisticated APS spraying technology (*e.g.*, automized mass flow meters, full PLC Siemens (Munich, Germany) S7 control, and temperature determination by high-resolution thermographic camera), coatings were deposited and analyzed with regard to phase composition, microstructure, residual stresses, and important thermal and mechanical properties. The results are used to optimize the powder fabrication route as well as the thermal spray process itself.

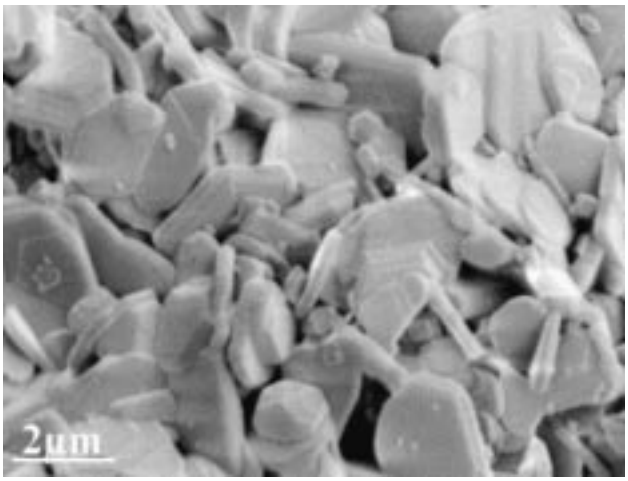

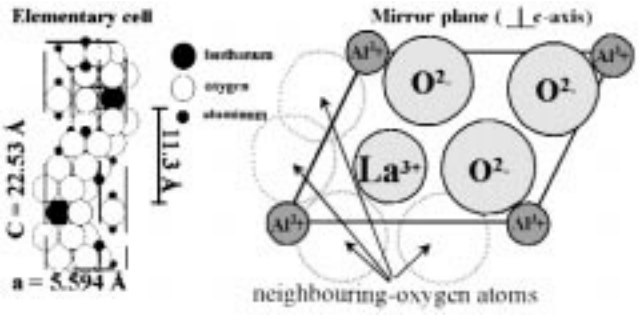

Fig. 2 Above: Platelet structure of the calcined oxide granulate. Below: Mirror plane projection (right side and vertical to the *c*-axis) and elementary cell (left side, big black dots: La^{3+}, little black dots: Al^{3+}, and white dots: O^{2-}) of lanthanum magnetoplumbite[5]

Table 1 Specific properties of lanthanum aluminate and commercial zirconia

Property	La-MP	Zirconia
Density (g/cm^3)	3.9–4.2	5.95
Thermal expansion ($10^6 \times K^{-1}$)	9.5–10.7	10.8–11.6
Thermal conductivity (W/m K)	0.8–2.6	0.6–2.3
Young's modulus (N/mm^2)	127	242

2. Powder Processing

The initial stage of the process is the fabrication of a fine-grained "raw powder" with the desired stoichiometry

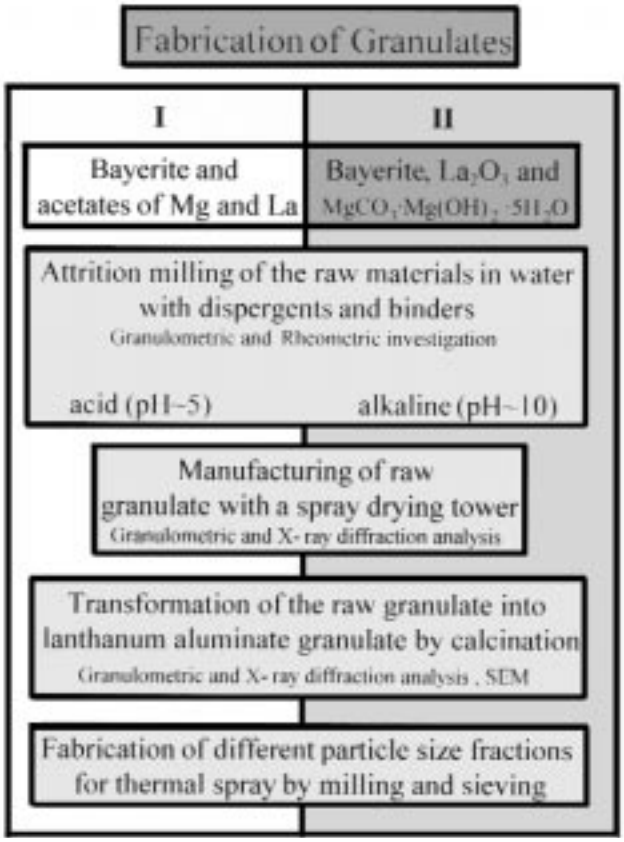

Fig. 3 Flowchart for the powder fabrication process

Table 2 Product name, source, and some specific properties of additives and raw materials

Material	Source	Amount (wt.%)/ oxide	pH	Average grain size d_{50} (μm)
Bayerite	Condea(a)	64/Al_2O_3	6	13
La_2O_3	Ampere(b)	99.9/La_2O_3	10	41.8
$La(CH_3COO)_3$				
$MgCO_3 \times Mg(OH)_2 \times 5H_2O$	Th.Geyer(c)	40/MgO	9	5.9
$C_4H_6MgO_4 \times 4H_2O$				
ZrO_2	Degussa(d)	. . .	. . .	. . .
Trusan 440	Trukem(e)	. . .	5	. . .
Trusan 480	Trukem	. . .	10	. . .
Trucor 830	Trukem	. . .	8–9	. . .
Trucor VP 9508	Trukem	. . .	8	. . .

(a) Condea Chemie GmbH (Hamburg, Germany)
(b) Ampere GmbH (Frankfurt, Germany)
(c) Th. Geyer GmbH (Renningen, Germany)
(d) Degussa-Hüls AG (Frankfurt, Germany)
(e) Trukem GmbH (Worms, Germany)

($LaMgAl_{11}O_{19}$). For this purpose, lanthanum and magnesium acetates, formates, or different oxide raw materials (hydroxides and hydroxy-carbonate) were used. Bayerite was used as the alumina raw material, which, if calcined, provides an intermediate cubic stage that thermodynamically favors the formation of the magnetoplumbite structure. A list of the raw materials is given in Table 2.

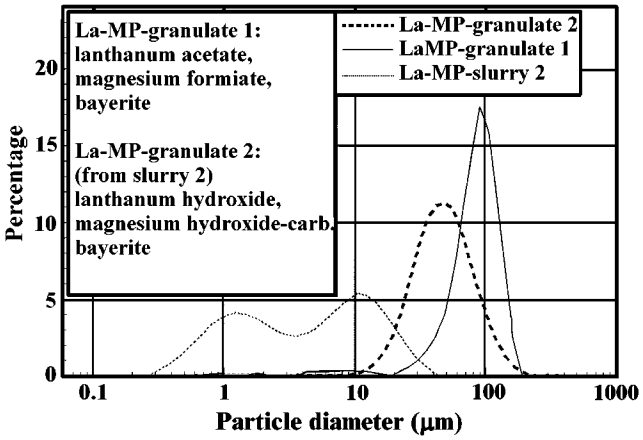

Fig. 4 Particle-size distribution of different slurries and granulates for the fabrication of lanthanum magnetoplumbite powder

The raw materials were intensively mixed and attrition milled with different dispergators and binders from Trukem. Afterward, the slurry was spray dried in a laboratory spray drying tower (Nubilosa GmbH&Co, Konstanz, Germany). The resulting spray-dried powders were thermally treated (calcined) in order to transform the raw mixture into lanthanum magnetoplumbite granulates (Fig. 3). For thermal spraying, different particle fractions were prepared to optimize the flow behavior.

In the first experiments, the slurry was fabricated with lanthanum acetate, magnesium formate, and bayerite using an acid dispergator in combination with an alkaline binder. The pH value was about 5.7.

To improve the rheological properties of the slurry as well as the particle shape and the mineral composition of the resulting granulate lanthanum oxide, magnesium-hydroxy-carbonate and bayerite were used in further experiments. The lanthanum oxide has to be treated with an ultrasonic device before mixing in order to transform it into hydroxide ($La(OH)_3$). This is necessary since this reaction is exothermic and leads to a rapid heating of the slurry. Without this step, a destruction of the temperature sensitive dispergators can occur.

Despite the improved properties, the water and additive content of the resulting slurry was quite high (water:solid = 65:35%). Alkaline dispergators and binders were used as additives. The pH value was about 10. At first, the mixture was only dried in an oven at 110 °C and treated with a mortar. To fabricate a powder with better flow characteristics and controllable particle size distribution, the slurry was spray dried at 92 °C (inlet temperature: 224 °C) with a feed rate of 20 mL/min.

2.1 Characterization of the Spray Granulate

To investigate the structure of the granulate as well as the chemical and mineral composition, scanning electron microscopy (SEM) and x-ray diffraction (XRD) were used. Additionally, the particle size distribution of the slurry and of the granulates was analyzed with a laser granulometer.

Particle size distribution patterns of the granulates before calcination from acetic and hydroxide slurries, and one hydroxide slurry with a bimodal particle size distribution, are shown in Fig.

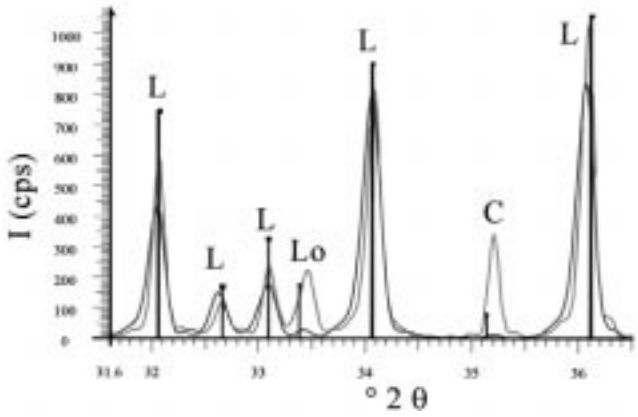

Fig. 5 Qualitative XRD patterns (extract) of calcined granulates, calcined for 4 h at 1650 °C, gray: acetic powder, black: oxide powder, L: LaMgA1l1O19, Lo: LaAlO3, and C: corundum

4. The peak of around 1 μm of the hydroxide slurry is caused by the lanthanum compound ($La(OH)_3$, as discussed above). The granulate based on the hydroxide slurry has a more regular particle size distribution and a lower maximum value (approximately 45 μm).

The XRD patterns of the "acetic" and "hydroxide" granulate calcined at 1650 °C for 4 h show that a complete transformation into the $LaMgAl_{11}O_{19}$ phase occurs only for the latter. In the acetic-based powder, additional phases such as $LaAlO_3$ and Al_2O_3, were present (Fig. 5). However, to investigate and determine the degree of crystallization, further XRD measurements have to be carried out.

The SEM images of the two calcined granulate types show again that only the hydroxide-type granules have a round shape (Fig. 6). This granulate consists nearly completely of crystallized little platelets. Cross sections of the acetic-type granules demonstrate that such granules can have a noncrystallized core. This has to be proved for the hydroxide type as well, although the XRD patterns suggest a crystalline phase.

3. Coating Deposition and Characterization

Atmospheric plasma spraying is an established way to produce TBCs. As a result of the high thermal and kinetic energy, this technology is expected to be appropriate to process the manufactured La-MP powder. The quality of a thermally sprayed coating with regard to microstructure, porosity, hardness, and other mechanical and electrical properties can be varied widely by tuning such spray parameters as supplied energy, substrate preheating, and process cooling. Also, the physical properties of coating materials (thermal expansion coefficient, α; heat capacity, c_p; and thermal conductivity, a) are finally influenced by the coating microstructure and porosity. Adequate deposition conditions have been worked out.

In this work, the sieved La-MP powder was used for the APS spraying process. A GTV P2000 console (GTV GmbH, Luckenbach, Germany) with a F4 plasma torch and a MARK IV powder feed unit (GTV GmbH, Luckenbach, Germany) were used, and all coatings were deposited onto $50 \times 50 \times 3$ mm^3 steel substrates (St12.03) using a meander (5 mm per step and 90 mm wide) movement of the plasma torch. The spray parameters were varied by using plasma powers of 36 and 43 kW, by using two different preheating temperatures of the substrate, and by using simultaneous cooling (air and CO_2).

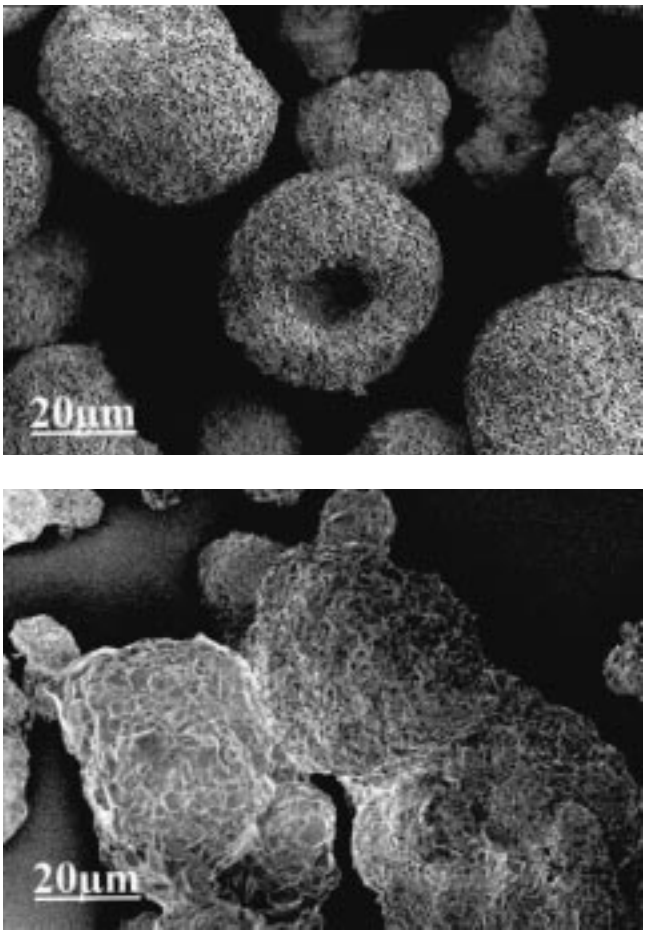

Fig. 6 SEM-SE images of the oxide (above) and the acetic (below) granulate

The coatings were analyzed with respect to their residual stress, microstructure (cross section, porosity, and density), phases (XRD), mechanical properties (microhardness and surface roughness), and thermophysical properties (coefficient of thermal expansion (CTE), heat capacity c_p, and aging characteristic).

3.1 Residual Stresses

Residual stresses can reach a critical value and cause failure of the coating; microcracks and delamination occur.[10] The final residual stress situation is influenced by the substrate preparation, thermal spraying, and composite postprocessing. The stress situation in the composite should be controlled during the spraying process in order to achieve minimum stresses in the layer composite under operation and load conditions.

The residual stresses in the coatings were determined by the microhole drilling method (Fig. 7). A plasma energy of 36.0 kW and the acetic granulate were used to deposit the APS coatings with a thickness of 100 μm (± 15 μm).

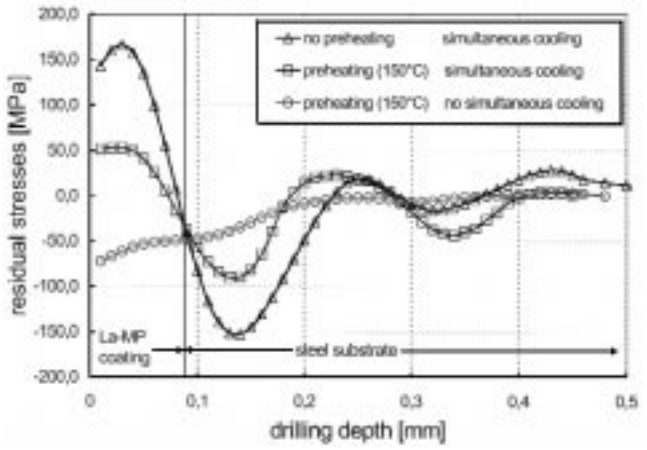

Fig. 7 Influence of the preheating temperature and cooling conditions of APS-deposited La-MP on steel (measured with the microhole drilling method)

As expected, the stress in the coatings depends strongly on the deposition conditions. In the coating, both tensile and compressive stresses are present.

A residual stress comparison among the three coatings clearly indicates the following correlation. High tensile stress is formed in the coating if simultaneous cooling is used during deposition. By preheating the substrate, the tensile stress could be reduced. By turning off the cooling during deposition, even a compressive stress in the ceramic coating could be achieved, but the temperature load of the substrate increases. The maximum temperature during the APS process was measured by a thermographic camera. It increased from 140 °C (no preheating and simultaneous cooling) to 340 °C (preheating and no cooling). During cooling of the composite from a higher uniform temperature level, larger compressive thermal stresses are induced in the coating and interface zones due to the mismatch of the CTE between coating (α_{La-MP} = 7 to 10 × 10^{-6}/K) and substrate (α_{steel} = 12 to 16 × 10^{-6}/K).

The stress situation in the substrate is quite different. In the first 100 μm beneath the interface zone, compressive stresses always appear, which are induced by the grit blasting process, a necessary pretreatment of the substrate. With increased thermal energy input into the substrate, the compressive stress in the substrate is relaxed.

3.2 Thermophysical Material Properties

The thermophysical properties of TBCs are important to predict the performance of the coating. The examinations presented in this section were done on APS-sprayed coatings using the acetic powder.

The heat conductivity (λ) of the coating was calculated by the product of density, heat capacity, and thermal conductivity (α):

$$\lambda = \rho \times c_p \times \alpha$$

The density ρ = 3.85 g/cm³ of the coating was determined by the principle of Archimedes. The temperature conductivity was determined by the laser flash method. It increases with temperature from α_{RT} = 0.005 cm²/s at room temperature up to α_{1200} = 0.066 cm²/s at 1200 °C. The heat capacity (c_p) was determined thermoanalytically (Fig. 8).

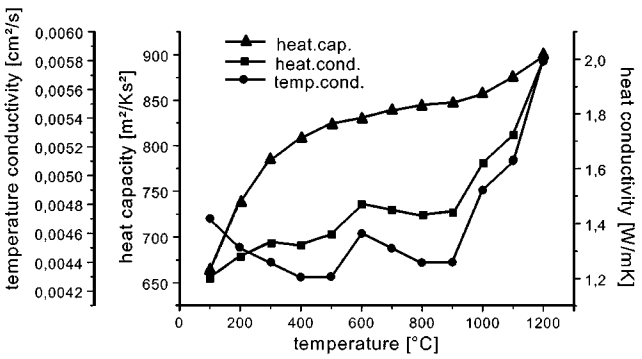

Fig. 8 Thermophysical properties of an APS-sprayed La-MP coating

Table 3 Dependency of the CTE of APS-sprayed La-MP

Temperature (°C)	CTE La-MP × 10^{-6} (1/K)	Ytrria PSZ × 10^{-6} (1/K)
100	7.7	10.0
300	8.1	11.1
500	8.2	10.9
800	8.6	10.9
1100	9.0	10.9
1300	9.3	10.9

The CTE and the aging behavior of TBCs are very important material properties influencing the lifetime of coated components. Thermal expansion mismatches between substrate and coating materials, as well as aging of the coating, result in the development of residual stresses during thermomechanical loading. A state-of-the-art partially yttria-stabilized zirconia and a spray cone were manufactured by APS. Dilatometer measurements were performed on the prepared spray cones. The thermal expansion of the coatings between 100 and 1200 °C and the shrinkage of the material during 50 h at a temperature of 1300 °C were determined.

After the La-MP coating is heated to a temperature of 1300 °C for the first time, it shows a strong shrinkage of up to 1.7% between 800 and 900 °C and of 0.3 % between 1100 and 1200 °C. These are irreversible processes because, during cooling, the volume decreases almost linearly with temperature. Phase analysis before and after heat treatment indicates that crystallization takes place, and the peak intensities of the XRD analysis are about double. The CTE is determined on the cooling leg. The CTEs of the PSZ and the LA-MP are listed in Table 3. The CTE of La-MP is slightly lower than the CTE of PSZ over the entire examined temperature range, but with increasing temperature, the difference between the two CTEs decreases due to the stronger temperature dependency of the CTE of La-MP.

The results of long-term aging (50 h) at 1300 °C are shown in Fig. 9. The thermal-sprayed La-MP material seems to fulfil the predicted low aging property. The volume loss of La-MP at the end of the experiment is about eight times less than that of PSZ. The change of volume of the La-MP is extremely small. It even seems that, during the experiment, the volume increases

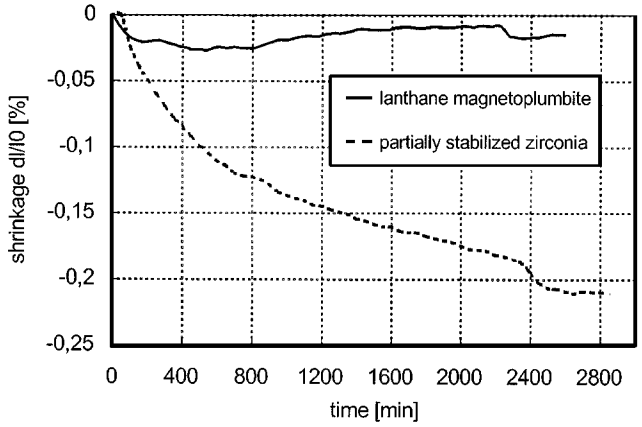

Fig. 9 Comparison of the aging behavior of APS-sprayed La-MP and PSZ at a temperature of 1300 °C

Table 4 Microhardness and indentation modulus

Property	Coatings La-MP	PYZ
HV 0.005	4300–5600	6300
E/(1-υ2)	120–140	160

slightly, probably due to the formation or growth of the platelets in the coating.[5]

Another very important property of thermal-sprayed coatings is the thermal shock resistance. Thus, samples for the determination of the thermal shock resistance were sprayed, but these results are not available yet.

3.3 Mechanical Coating Properties and Phase Analysis

The surface roughness of the coatings was determined with a tactile method. The coefficient of surface roughness R_z ranges from 30 to 90 μm, influenced mainly by the grain size distribution of the used granulate.

The porosity of the coatings was determined by light microscopy. It is in the range of 5 to 10%. The porosity is influenced by the specific energy of the plasma and the grain size distribution of the powder.

The elastic and plastic deformation behavior of the TBC coating is important to predict the behavior of the coatings during application. The microhardness and the indentation modulus describe these behaviors. A high hardness improves the resistance of the material to indention by a mechanical load. A low indentation modulus is to be favored, since stresses induced by deformation of the composites decrease with a lower modulus of the ceramic coating.

All of the deposited coatings were widely examined with respect to plastic and elastic deformation behavior with Fischercope® (Sindelfingen, Germany) universal microhardness test equipment (F = 500 mN). The ranges of the microhardness and the indentation modulus of the examined La-MP coatings as well as the values for APS-sprayed yttria-stabilized PSZ are presented in Table 4. The microhardness of all La-MP coatings is higher than that of hardened steel but is below the hardness

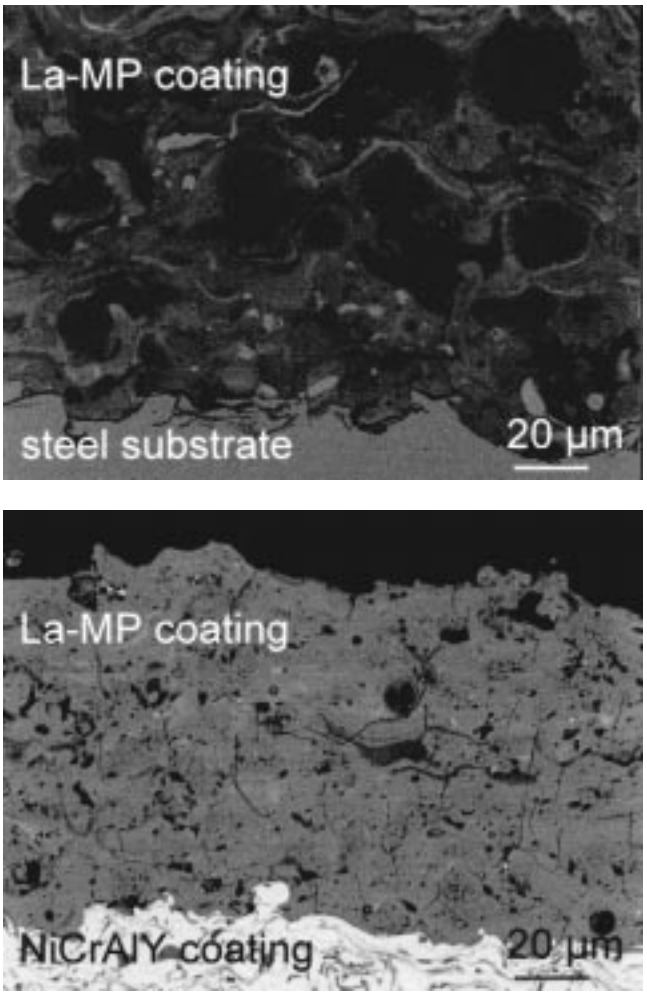

Fig. 10 Typical BSE analysis of APS-sprayed La-MP coatings using acetic (above) and oxide (below) powders

of zirconia. The elastic behavior of all La-MP coatings is superior to PSZ because of the lower indentation modulus.

The microstructure of the thermally sprayed coatings is analyzed in polished and etched cross sections. In many coatings, unmelted or just partially melted particles can be found, and pores with a diameter of up to 35 μm are observed. A high specific plasma energy and fine grain size are necessary to fully melt the particles and to achieve a fine, homogeneously distributed porosity.

The microstructure of the coatings produced with acetic powders and the ones using the hydroxide powder differ with respect to the distribution of the elements. The heterogeneity of single acetic powder granulates could not completely be eliminated by thermal spraying and was therefore partially transferred into the coating. This heterogeneous elemental distribution is seen using backscattered electron microscopy (BSE) (Fig. 10). Electron probe microanalysis shows that the main part of the coating consists of stoichiometric La-MP (light gray), the darker regions are Mg-rich or even consist of pure alumina, and the light regions consist of La-rich compounds or ZrO_2. A good homogeneous elemental distribution in the coatings was reached

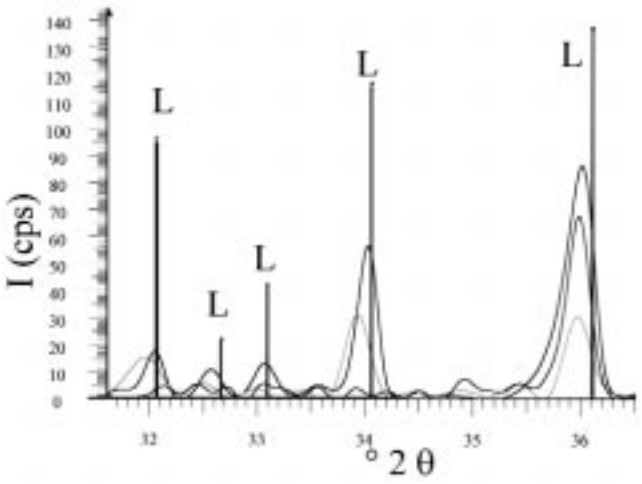

Fig. 11 XRD pattern of as-sprayed La-MP (L) coatings using powders calcined at 1650 °C for three different time periods: light gray—non-calcined powder, gray—30 min calcined; and black—30 h calcined

by using the broken oxide powder (Fig. 10). After etching the cross sections, typical platelets can be seen in some regions using microscopy. Other regions show no grain boundaries and seem to be noncrystalline.

The XRD patterns of the acetic coatings confirm that the coatings not only contain La-MP, but also other phases such as $LaAlO_3$ and MgO. It is important to mention that all XRD patterns show only very small peak intensities. Probably, similarly to mullite, La-MP has the tendency to build amorphous phases when deposited *via* thermal spraying.

Therefore, initial experiments were carried out to deposit high crystalline La-MP coatings. Three powders, manufactured *via* hydroxides, with different sizes of platelets were processed by thermal spraying. The XRD patterns of these three coatings show that the peak intensity increases by the use of powders with a large platelet size (Fig. 11). The grade of crystallization has to be investigated, *i.e.*, by further XRD measurements. The XRD patterns only show the desired crystalline phase La-MP.

4. Discussion and Conclusions

First coatings made of the acetic powder show promising thermophysical and mechanical properties in comparison to PSZ, even though the phase composition was not optimized. Residual phases such as Al_2O_3 and $LaAlO_3$ could be found. By optimization of the powder processing using oxide compounds, a coating of nearly pure lanthanum magnetoplumbite could be produced.

The La-MP powder still tends to form noncrystalline phases during the thermal spraying process similar to mullite. However, the experiments show that the grade of crystallization is improved using precalcined granulate.

It is expected that a homogenous and fully crystalline La-MP TBC can be manufactured by further optimization of the powder and deposition process. Due to the superior qualities of this new material, it seems probable that it will replace the conventional PSZ-TBC in the future.

References

1. G. Marci and G. Staniek: in *Kolloquium Wärmedämmschichten*, M. Peters, U. Schulz, U. Leushake, and W.A. Kaysser, eds., DLR, Institut für Werkstoff-Forschung, Köln, Germany, 1996, pp. 50-53 (in German).
2. R.L. Jones: *J. Thermal Spray Technol.*, 1997, vol. 6 (1), pp. 77-84.
3. J. Wigren and L. Pejryd: in *Thermal Spray: Meeting the Challenges of the 21st Century*, C. Coddet, ed., ASM International, Materials Park, OH, 1998, pp. 1531-42.
4. M. Streicher: Ph.D. Thesis, University of Karlsruhe, Karlsruhe, Germany, 1991 (in German).
5. R. Gadow and G. Schäfer: in *Ceramic Engineering and Science Proc.*, Ersan Ustundag, ed., 23rd Annual Conference on Composites, Advanced Ceramics, eds., Westerville, OH, 1999, vol. 20 (4), pp. 29-300.
6. R. Gadow and G.W. Schäfer: European Patent PCT/EP99/00982, 1999 (in German).
7. A. Kopp: *Ph.D. Thesis*, University of Stuttgart, Stuttgart, Germany, 1991 (in German).
8. T. Cosack and M. Thoma: *Wärmedämmschicht im Turbinenbau*, op. cit. Ref 1, pp. 20-22 (in German).
9. U. Dietel: Ph.D. Thesis, Technical University of Munich, Munich, Germany, 1995 (in German).
10. K. Berreth, M. Buchmann, R. Gadow, and J. Tabellion: in *Material Science & Engineering*, G. Kostorz, C.C. Koch, E.J. Lavernia, E. Werner, and M. Kato, eds., vol. A288, *European Material Conf.*, Straβburg, France, 1999, pp. 154-59.